"**The oxides and their surfaces at the DFT level: achievements and challenges**"

Sergio Tosoni

Abstract

This chapter illustrates the state of the art of computational approaches to simulate oxide materials and oxide surfaces at the DFT level. First, the most critical methodological issue is discussed: the calculation of excited-states related properties (Section 1) and the derivation of reliable structural model (Section 2), discussing pros and cons of the cluster and periodic approaches. Then, the chapter will focus on the description of the metal/oxide interfaces, a key-aspect in modelling heterogeneous catalysts (Section 3). In Section 4 the catalytic role of metal clusters supported on oxide surfaces is shown for some particularly relevant reactions.

1. Oxides: still an open challenge for DFT?

First-principles simulations ensure results of general validity and high predicting power since they do not rely on any empirical parameter. The accuracy of the results, however, may vary, depending on the specific type of chemical structure and the physical properties under investigation. The high computational cost of first-principles simulations, compared with molecular mechanics simulations, imposes limitations on the size of the structures that can be considered, or on the time scale of the dynamic simulations. The key aspect of such simulations, thus, is the balance between efficiency and accuracy.

Oxides are the main components of the earth crust, which underlines their relevance to environmental chemistry and geochemistry. Moreover, their potential technological applications span from heterogeneous catalysis to microelectronics, coating, photovoltaic, gas sensing and many others.

Despite the apparent chemical simplicity behind the concept of metal oxides, this is a wide class of compounds and materials, exhibiting different properties in terms of electronic structure, magnetic behavior, and chemical reactivity.[1] As we will discuss in the following, the accuracy in describing these various properties is still a significant challenge for nowadays computational methods.

Traditionally, the most relied methods to treat excited states are based on the multideterminal expansion of the wave function solution, going thus beyond the Hartree-Fock solution of the electronic ground state.

The different truncated Configuration Interaction (CI) expansions, especially the one including only single excitations (CIS), together to the more accurate MRCI or CASPT2 methods provide a direct way to approach excited states. However, one should be aware that, at the state of the art, this family of methods are widely applied for molecules, but their implementation for periodic systems is much less common, which poses a limit to their use in the case of oxides.

The most accurate way to approach excitations in the framework of DFT is its Time Dependent formalism, TD-DFT, based on the Runge-Gross theorems[2]. TD-DFT thus extends the standard formulation of DFT described above to time-dependent phenomena. In a few words, it consists in coupling a time-dependent operator to the reference non-interacting electron density at the base of DFT via the so-called Runge-Gross equations:

$$i\frac{\partial}{\partial t}\phi_i(r,t) = \hat{h}_{KS}(t)\phi_i(r,t) \qquad (1.)$$

where the Kohn-Sham one particle Hamiltonian and orbitals depend on the time and so does the density

$$\rho(r,t) = \sum_i \left|\phi_i(r,t)\right|^2 \qquad (2.).$$

The Coulomb external potential and the exchange-correlation potentials are then function of the time-dependent electron density, which evolves starting from the initial ground state. In all practical applications of TD-DFT, however, an adiabatic approximation in time is adopted, stating that

$$v_{xc}\left[\rho(r,t)\right] = v_{xc}^{gs}\left[\rho\right]_{\rho=\rho(r,t)} \qquad (3.),$$

The exchange correlation potential of the ground state, in this approximation, does not change during the excitation process and is applied to the electron density evolving with time. This permits to use all the approximations implemented in standard static DFT codes for ground state calculations in the TD-DFT formalism.[3-5]

TD-DFT appears to be more robust that CIS based on a HF reference[6] and profits of a relative computational simplicity compared to wave-function methods. In the recent years, it has been widely and successfully applied to periodic systems.[7-9]

Optical transitions, absorption and emission phenomena in oxides and semiconductors, are often approached as energy differences between one-electron energy levels extracted from the band structure obtained by either HF or DFT methods. The application of hybrid functionals to the study of the electronic structure of oxides and other strongly correlated solids provides a notable improvement over the description arising from GGA, strongly affected by the self-interaction error.[10-16] Nevertheless, remarkable errors still resulted by applying widely used hybrid functionals such as PBE0, B3LYP or HSE to the specific class of two-dimensional or layered oxide materials.[17] In this case, it is beneficial to tune the percentage of Fock exchange included in the functional specifically for each oxide, depending on its dielectric constant.[18-20]

The introduction of a part of the Fock exchange is not the only strategy to improve the description of the band gap in oxides and related material where LDA and GGA fail even qualitatively. A commonly used approach is to add two parameters to the LDA or GGA exchange correlation functional with the idea to mimic an effective onsite Coulomb (U) term, as in the Hubbard model, and an exchange (J) term between electrons with the same orbital angular momentum.[21,22] The resulting method is often referred to as DFT+U, or, more specifically, as LDA+U or GGA+U. One advantage of LDA+U or GGA+U over the hybrid functionals described above is the lower computational cost. Nevertheless, the determination of the Hubbard parameter should be done with some care, in particular if the choice relies on empirical criteria rather than on a self-consistent procedure.[23-25]

2. Oxide surfaces: structural models

As mentioned before, oxides are a wide class of materials, whose chemical bonds span from highly ionic to polar covalent. Whenever relevant ionic interactions are present, long-range electrostatic effects play an important role and cannot be neglected. This rules out the possibility to perform simulations on chemical properties of oxide surfaces by simply cutting out a region representative of a surface site from the crystal lattice, even if a chemical reaction (in terms of bond breaking and forming) can be seen as a rather local effect. In practice, one may choose to represent the oxide surface either by choosing a properly embedded cluster model or a suitable supercell periodic approach. The latter is rather straightforward although it prevents the application of wave-function methods.

The design of an embedded cluster model for this surface begins by defining the so-called quantum region and the external embedding zone. The quantum region is composed by the ensemble of atoms whose electrons are explicitly treated in the first-principle simulation. This region will be surrounded by a buffer zone, whose function is to enforce mechanical boundaries on the atoms of the quantum regions, as well as account for the short-range Coulomb forces, long range Coulomb effects, and long range polarization. The quantum region necessarily includes the atoms that play a fundamental role in the property under study. Thus, it should be large enough to accommodate any possible adsorbate or to contain the atoms involved in the electronic transitions of interest. Clearly, the larger the quantum region, the better the representation of the surface, but the larger the computational cost as well. Such an approach has been used

for long time to study the surface properties of the paradigm of ionic oxide surfaces, namely MgO(100).[26-28] As a general rule, the local quantum region contains the atoms directly involved in the property under study and the first shell of atoms around those centers. In any case, one should always check that the property of interest is converged with respect to the size of the quantum region.

Then, it is necessary to consider the short-range electrostatic repulsion between the atoms in the quantum region and those surrounding them. Here, quantum contributions are still important and should be properly accounted for. The Total Ion Potential (TIP) embedding[29,30] and the more rigorous Ab Initio Embedding Model Potential (AIEMP) scheme[31,32] recently improved to better describe the Pauli repulsion term[33] are particularly worth being cited. Both embedding schemes incorporate the interaction of the quantum cluster electrons with the surroundings into an effective 1-electron Hamiltonian at a low computational cost.

Despite the inherent short-range nature of quantum interactions, the presence of ions in the surroundings play a non-negligible role. This effect can be effectively modeled by calculating the Madelung field of the ions not included in the quantum region and adding this potential to the cluster Hamiltonian. To this purpose, the exact Madelung field is first calculated by an Ewald summation[34] with formal point charges at the lattice positions. The external boundary regions of the point charges array is modelled in such a way that the overall neutrality of the model is ensured.[35-39]

The adsorption of atoms, molecules or metal clusters on the surface of an oxide can cause a long-range response of the crystal to changes in the electronic structure of the quantum region induced by the adsorbate. This can be done by adding the polarization contribution to the total energy ((E_{pol})), as formerly derived by Born:[40]

$$E_{pol} = -\left(1 - \frac{1}{\varepsilon}\right)\frac{q^2}{2R}, \qquad (4.),$$

where □ is the dielectric constant of the material, q is the absolute value of the charge and R is the radius of the spherical cavity in which the charge is distributed. To avoid any ambiguity in the definition of R, one can rely on the so-called shell models,[41 42] which allows treating the cluster electronic structure and the lattice polarization in a self-consistent way,[43-45] or as direct option to simulate a polarizable environment.[46-53]

The category of oxides, however, is much wider than the case of ionic compounds such as MgO. Cutting a portion of a covalent (or partly covalent) oxide, such as SiO_2, TiO_2, ZnO or CeO_2, poses different challenges.

In some cases, the bonding between oxygen and other atoms in the oxide structure is highly directional (for instance in SiO_2) and cutting a cluster from the bulk necessarily results in the presence of dangling bonds. In these cases, a simple embedding consists in saturating the cluster dangling bonds by H atoms.[54-56]

The saturation of the cluster broken bonds is an important aspect of the embedding, but not the only one. In fact, in this way long-range electrostatic and polarization effects are totally neglected, which is not the ideal solution for materials such as ZnO or TiO_2 or zeolites. Here, one can couple the quantum region with a larger external zone treated by means of empirical molecular mechanics force fields (QM/MM),[57] in particular by the Integrated Molecular Orbital Molecular Mechanics (IMOMM)[58] or ONIOM[59] methods. The main problem consists in defining the interface between both regions, which is made precisely by saturating the dangling bonds with hydrogen atoms. In this sense IMOMM and ONIOM methods permit one to handle large models and to include all important effects of the crystal. This strategy has been successfully applied to the study of metal-support interactions in silica[60] and reactivity of zeolites[61-74] and more in general in catalysis.[75]

Despite the relevance of embedded cluster methods, in particular related to complement or benchmark DFT calculations with more accurate calculations at the post Hartree-Fock level, most of the simulations of oxide surfaces is nowadays performed recurring to periodic slab models. The idea behind the slab model is to define a periodic unit cell exhibiting the crystal surface of interest and to include in the unit cell a finite number of atomic layers in the direction perpendicular to the surface, while periodic symmetry is used to replicate the unit cell in the directions parallel to the surface.

The area of the unit cell of the slab is tuned depending on the phenomenon of interest: it should be large enough to host adsorbates or supported metal particles for instance, or allow for the diffusion of atoms and molecules on the surface. The number of atomic layers in the slab should be large enough to ensure that a realistic bulk region is present underneath the surface: this is done by checking the convergence of some paramount property (e.g. the surface energy, or the band gap) with respect to the number of layers. Many efficient and parallel computer codes such as VASP,[76-78] CASTEP,[79] ABINIT,[80,81] Quantum Espresso,[82] to mention a few, relies on this type of periodic approach. The aforementioned codes use plane waves as basis set and, since these functions are intrinsically periodic, it is necessary to replicate the slab model in the third direction as well leaving a sufficiently large vacuum region between the interleaved slabs. The use of a repeated slab is not necessary when adopting local basis sets such as the Gaussian Type Orbitals (GTO), as in most quantum chemical codes, for instance in CRYSTAL.[8]

From the discussion above, it appears that the periodic slab model is really appealing, but care should be applied when the structure is not centrosymmetric, i.e. the upper and lower faces of the slab differ. This creates a macroscopic spurious dipole when the cell is replicated in the non-periodic direction, as in the plane-waves approach. Specific techniques are in use to avoid artefacts, for instance by adding a counter-dipole in the empty space region.

3. Oxide-metal interfaces at the keys of heterogeneous catalysis

Many industrial chemical processes, from fine chemical synthesis to combustion control, relies on catalysts to improve their yield and sustainability.[83] The relevance of catalysis to our society can only increase in the near future, if one considers the ambitious goals of the European Green Deal. In this context, the capture and reuse of greenhouse gases such as CO_2 or CH_4 represent a crucial task. In many cases, the catalytic devices actually in use fall in the domain of heterogeneous catalysis.[84] The prototype of a heterogeneous catalyst is a metal particle in the scale of hundreds/thousands atoms dispersed on a carbonaceous or oxidic support.[85,86] The dispersion and the size-reduction of the metal particles are a key-aspect in determining their activity: in contrast to the bulk, particles in the nanoscale and below exhibit peculiar electronic and structural features affecting their reactivity. For instance, small gold aggregates are very active, contrary to the mostly inert bulk Au.[87-89] In small particles, a large share of the atoms lies at the interface with the support, which can remarkably affect their chemical properties and stability.[90] In some cases, the metal-support interaction is strong[91-93] and the catalyst is significantly influenced.[94,95]

Based on these considerations, it is understandable that the computational characterization of metal aggregates supported on oxides represents a topic of paramount interest. Given the huge amount of computational work, making a comprehensive review undoable, this section focuses specifically on the case of gold, where the activity of small clusters and nanoaggregates is most striking with respect of the noble character of the bulk.[96]

More specifically, we will treat the complicated trends in Au adsorption energy spanning over different oxides (Section 3.1), the role of point defects as nucleation centres (Section 3.2), the peculiar properties of gold/oxide interfaces (Section 3.3), and the Au deposition on ultrathin oxide supports (Section 3.4).

3.1 The quest for rational trends in Au/oxide interactions

The smaller, the more active? Even though this can be an oversimplification, it is fundamentally true that the particle size is a key-factor in determining the catalytic activity of nanometric and subnanometric gold particles.[97,98-102] At the normal operating conditions in heterogeneous catalysis, however, the dispersed supported nanoparticles are subject to aggregative forces, which may lead to sintering, i.t. the formation of bulky and inactive particles, with a remarkable wase of precious metal. Two processes are at the base of sintering: i) particle migration and aggregation, and ii) the so-called Ostwald ripening process, which consists in the loss of single atoms from smaller aggregates toward larger ones.[103,104] Many strategies have been applied to contrast thermal deactivation of gold catalysts, spanning from alloying of the Au nanoparticles with non-noble transition metals,[105,106] to the employ of organic ligands to promote redispersion

on the surface.[107] Nevertheless, the first factor to take into account to prevent sintering is the gold adhesion strength to the oxide surface: if the Au particles adhere strongly, they will better withstand the catalytic operating conditions without undergoing aggregation. A general and simple rule to predict the Au adhesion on various oxide surfaces, however, has not yet been found. A study by Hemmingson and Campbell presents a meta-analysis of calorimetric and morphological measurements of metal nanoaggregates on various oxide surfaces.[108] As far as the behaviour of the metal composing the supported particles is concerned, it can be stated that the adhesion energy of a given metal on a defect-free oxide surface scales with the oxophilicity of the metal.[109] DFT calculations of single transition-metal atom adsorption on oxides support this model, because the main contribution to the binding energy is due to the metal-oxygen interaction.[109-114] On the contrary, the trend in adhesion energy of a given metal on various oxide surfaces is more difficult to rationalize. In the specific case of gold, an interesting an interesting finding is reported in Figure 1:[108]

MgO(100) ≈ TiO_2 (110) < □- Al_2O_3 (0001) < CeO_2 (111) ≈ Fe_3O_4 (111)

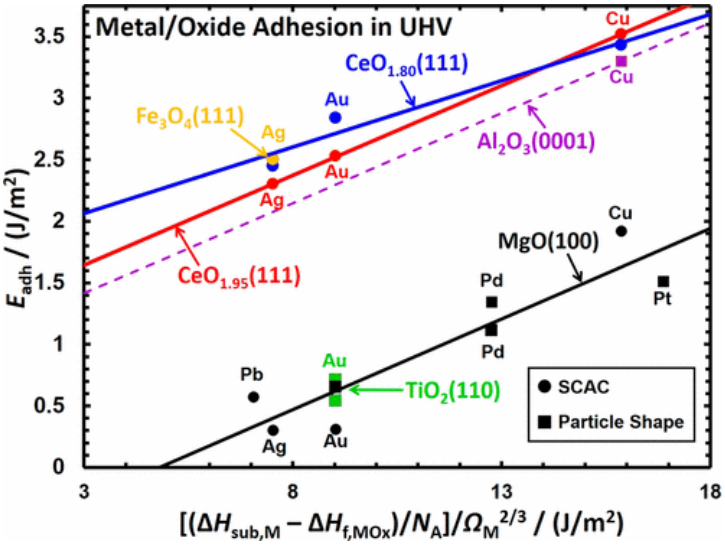

Figure 1. Experimental adhesion energies of various metals to various oxide surfaces plotted versus an estimate of the metal's oxophilicity. Reproduced with permission from ref. 108. Copyright (2017) American Chemical Society.

An intuitive and simple model to predict the adhesion of a metal on an oxide surface could be based on the chemical potential of the oxygen in the oxide lattice: i.e., the more an oxygen ion is bound to the lattice, the less it is prone to coordinate adsorbed aggregates. Accordingly, one would think that the energy necessary to remove an oxygen ion from a surface lattice site is a good descriptor of the oxide's capability to bind metals, like gold. This model, however, cannot explain why titania (covalent and quite reducible) and magnesia (strongly ionic and not reducible) bind gold with substantially comparable adhesion energies. This puzzle can be recomposed recurring to dispersion-corrected DFT calculations on the adhesion energy of gold nanoparticles on magnesia, titania, and ceria.[115] Three forms of gold deposits were considered, an isolated atom, two isomers of the Au_{20} nano-clusters (see Figure 2), and a periodic extended interface that better represents a large gold particle.

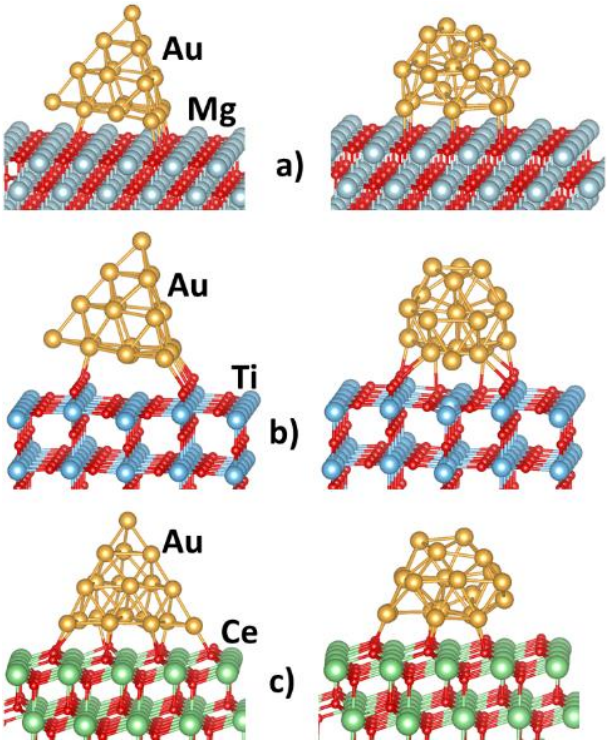

Figure 2. Pyramidal and fcc Au_{20} isomers adsorbed on a) MgO (100), b) TiO_2 rutile (110) and c) CeO_2 (111). Picture reproduced with permission from ref. 115. Copyright (2017) American Chemical Society.

The adhesion energy of a single gold atom (preferentially on oxygen) resulted to be similar for the three oxides, namely circa 1 eV, with a relevant contribution from long-range dispersion (in the order of 20-25%). No change in the electronic configuration of Au were detected. For Au_{20} a trend in adhesion energy emerged between the three oxides, namely CeO_2 > MgO > TiO_2. For the extended interfaces, the trend found in adhesion was CeO_2 ≈ MgO > TiO_2. The reason for the scarce adhesion of Au on titania was mostly ascribed to morphological factor (such as the zigzag profile of the rutile (110) surface), preventing a close interaction with larger Au aggregates. However, a model based barely on morphological factors would not be able, either, to fully explain the observed trend, i.e. the adhesion energy of gold nanoparticles following the trend CeO_2 > MgO ≈ TiO_2.

A key-factor in reconciliating theory and experiment is to account for the presence of point defects such as oxygen vacancies on the oxide surfaces. These defects act as preferential nucleation and binding sites for deposited nanoparticles, increasing remarkably the binding of single Au atoms and clusters. Clearly, this holds true for ceria, or titania, where oxygen vacancies are inherently present in the lattice. Oxygen vacancies in an ionic oxide such as MgO are much less common, though very reactive. We can thus speculate that the gold-oxide adhesion puzzle is a complicate scenario where many factors play a role, from the surface's corrugation and morphology to the match between gold lattice and oxide's oxygen anions sublattice. Very important is, however, the role played by point defects such as oxygen vacancies in binding the metal nanoparticles.

3.2 Point and extended defects as nucleation centres

Point defects on oxide surfaces are important not only under the point of view of their reactivity and enhanced binding capability to bind adsorbates, but also because they can trigger charge transfer processes which, in turn, alters the reactivity of the adsorbed atoms or aggregates. While metal surfaces, characterized by a high degree of electron delocalization, provide an almost uniform potential energy landscape to coordinate metal adatoms, adsorption and nucleation on oxide surfaces is substantially influenced by the presence of point defects.[116-117] In the case of F-centres on MgO(100), for instance, the calculated binding energy of Au atoms increase by a factor 3.[118] The role of F centres on MgO (100) in stabilizing and activating gold adducts via charge transfer was also proven for small clusters. [119, 120]

Even on oxides such as titania, where oxygen vacancies are easier to form, a strong effect on the coordination of metal atoms and aggregates is observed, for instance in the case of rutile (110).[121] Despite the general electrophilic character of gold, however, the transfer of the trailing electrons associated with the oxygen vacancy in rutile to the supported Au cluster does not always take place, depending on the orientation of the Au orbitals and their overlap with the Ti(3d) orbitals hosting the electron charge near the oxygen vacancy.[121]

Depending on the support, the role of defects as preferential adsorption sites is not limited to the cases where these are located at the surface.[122]

The effective role of point defects in promoting dimerization of Au adatoms was proven by means of DFT calculations for the case of non-bridging oxygen defects on hydroxylated quartz.[123]

Doping with non-isovalent elements can also induce the enhancement of the Au adhesion energy, as well as charge transfer. This has been shown for the case of transition metal atoms doping (Cr, Mo, Nb) of simple oxides such as MgO or CaO.[124-126] In particular, Mo-doped CaO, CaO_{Mo}, and undoped CaO films have been prepared and their adsorption properties have been studied experimentally and theoretically by DFT calculations. Deposition of Au at 300 K on pure CaO films results in the formation of 3D gold particles, indicating weak adhesion and small or no charge transfer between the metal and the oxide support. In contrast, on the doped CaO_{Mo} films Au forms flat 2D islands, as expected when the interaction is dominated by charge transfer from the support to gold.

3.3 The cluster-oxide contact region is a highly reactive zone

The adhesion of a metal adduct on an oxide surfaces influences more pronouncedly the chemical behaviour of those metal adatoms that lie at the boundary between the adduct and the oxide. The scarce accessibility of this region to most experimental surface science techniques makes the information provided by good quality simulations of outstanding value. However, modelling a metal/oxide interface is not an easy task.[127] Hybrid functionals outperform GGA methods in describing the electronic structure of most oxides, but sometimes show worse performances compared to standard GGA when treating metallic systems.[128-129] It must also be considered that the structural complexity of a metal oxide interface is a relevant constrain in choosing the computational approach. Nevertheless, the adoption of an adequate computational methodology is necessary to properly describe delicate phenomena such as charge transfer at the metal/oxide interface. This depends on the oxide's electron affinity and ionization potential with respect to the metal work function.

A first chemical phenomenon of interest at the metal/oxide interface is the reverse of what has been described in the previous section: while oxygen vacancies stabilize adsorbed metal particles, the presence of metallic aggregates on a on oxide surface can trigger the oxygen removal from the lattice at the metal-oxide interface and the subsequent migration (reverse spillover) of the oxygen atom on the metal particle. Even on a definitely non-reducible oxide such as MgO, the creation of an interface oxygen vacancy at the border of an Au cluster is facilitated.[130] Also on rutile TiO_2, as studied by Cheettu and Heyden,[131] the presence of Au dimers or trimers reduces the oxygen vacancy formation energy. On the same rutile surface, the V_O formation energy in presence of a supported Au nanorod was systematically investigated as a function of the vacancy-metallic rod distance.[90] It resulted that, for oxygen sites at direct contact (or in close proximity) to the metallic Au rod, the formation energy decreased by more than 30%.

4. Supported Au particles in computational heterogeneous catalysis

After the description of the problem from the perspective of the fundamental surface science, we can now review some examples of applications concerning the usage of supported Au catalysts in reactions of high relevance for green chemistry and exploitation of renewable resources, such as the CO oxidation to CO_2, the water gas shift (WGS) reaction, and the CO_2 hydrogenation to methanol.

4.1 CO oxidation

CO oxidation over titania-supported gold nanoparticles is perhaps one of the most studied reactions in computational catalysis.[132] Nevertheless, the mechanism is still under debate. In a Langmuir-Hinshelwood (LH) type of mechanism, CO and oxygen molecules are assumed to adsorb at the same time on the surface, diffuse, and reach the catalyst. The gold particle binds strongly CO, while the interatomic bond of the O2 molecule is weakened at the cluster-oxide interface.[133-136] CO can then react and bind an O atom of the activated O_2 molecule forming CO_2 and an adsorbed O ad-atom, overcoming a low barrier. A second CO molecule binds to the Au catalyst and reacts with the O ad-atom to form CO_2. However, the relatively low desorption temperature of oxygen (170 K) rules out this mechanism at room (or higher) temperatures.[137]

An alternative mechanism is the so-called Mars-van Krevelen (MvK), where the active O species reacting with CO are actually coming from the lattice of the supporting oxide. This was proven experimentally dosing CO in an oxygen-free atmosphere on an Au/TiO_2 catalyst.[138] The vacancies are then refilled by dosing oxygen, closing thus the cycle. Interestingly, both the catalytic activity and the capability to store oxygen scale linearly with the Au/TiO_2 perimeter, thus showing the pivotal role of the cluster/oxide interface.

The direct role of the lattice oxygen atom in the MvK mechanism suggests that the chemical nature of the supporting oxide is very important: in particular, the reducibility of the oxide, implying that the formation of oxygen vacancies has a lower thermodynamic cost, are good candidates to support gold particles for the CO oxidation reaction. Indeed, a direct correlation between the activity of the supported Au nanoparticles and the reducibility of the supporting oxide was proven, thus validating the MvK mechanism.[139-141] Note that no reaction occurs on the bare surface in absence of Au nanoparticles.

The MvK mechanism for CO oxidation over Au/TiO_2 has been the object of several computational studies. Li et al.[142] performed Born-Oppenheimer molecular dynamics (BOMD) simulations to compare the CO oxidation on Au_{16} and Au_{18} clusters supported on the titania rutile (110) surface. They found that titania lattice oxygen atoms are more accessible for CO adsorbed at the Au_{16}/TiO_2 perimeter compared to a closed-by adsorbed O_2 molecule. The whole proposed catalytic cycle is sketched in Figure 3. The key steps of the MvK cycle are the removal of the lattice oxygen atom (barrier of 0.2 eV) and the splitting of the O_2 molecule to refill the vacancy (0.3 eV). For comparison, the alternative LH mechanism is hindered by a substantially larger barrier (0.6 eV).

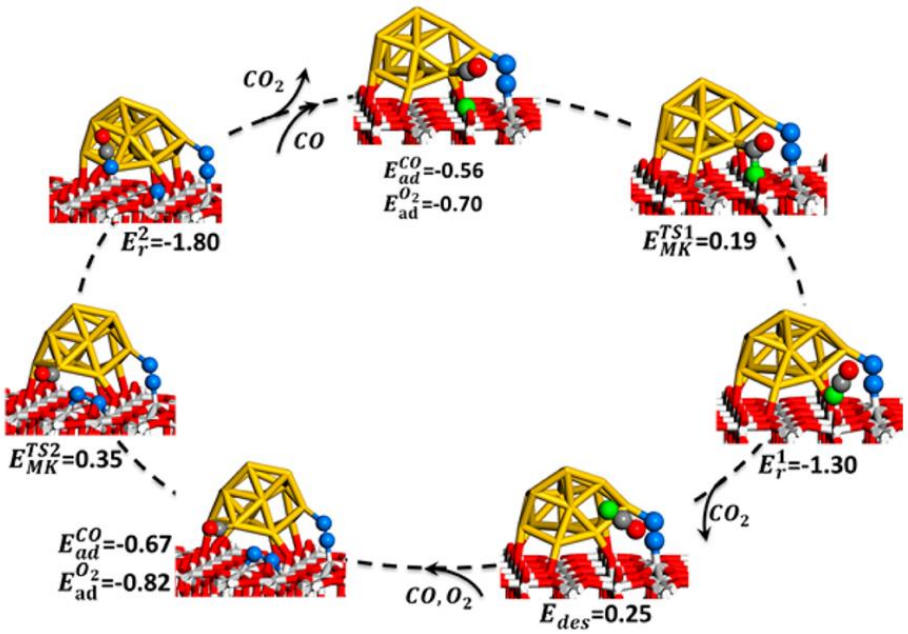

Figure 3. Reaction pathway for CO oxidation at Au_{16}/TiO_2 interface, following the Au-assisted MvK mechanism. E_{ad} (eV) represent adsorption energies and E^{TS} (eV) represent the reaction barriers for the generation and refilling of the oxygen vacancy. The negative and the positive values indicate exothermic and endothermic process, respectively. Reprinted with permission from ref. 142. Copyright (2014) American Chemical Society.

An intriguing finding is that, however, the LH mechanism becomes competitive over the slightly larger Au_{18} cluster, showing that the flexibility of gold clusters in the non-scalable regime largely determines their properties.[143]

In the case of a DFT+U study on a bulkier gold structure, such as a nanorod supported on titania rutile (110), a similar picture was obtained.[90] Upon adsorption and splitting of the O_2 molecule at the gold-titania interface, a very small barrier (0.24 eV) was found for the LH mechanism, while the removal of a lattice O had a barrier as large as 0.55 eV.

Saqlain et al. investigated by means of DFT+U calculations the role of Au_{10} clusters in facilitating the formation of surface oxygen vacancies on anatase (001).[144,145] Indeed, it was shown that, at the O lattice site at the border of the supported cluster, the formation of the vacancy becomes exergonic already at T > 230 °C. One can thus speculate that these cluster/surface border regions will be available to react according to the MvK mechanism. An interesting finding is that Au_{10} clusters are more active than smaller Au_3 aggregates; on the one hand, smaller aggregates are more flexible, and their atoms are in closer contact with the surface underneath, which should increase their activity. However, beside loosening the Ti-O bonds, Au supported clusters play another important action to promote the reduction of the oxide, namely taking part of the trailing electrons left by the removed oxygen on the oxide, contributing to the stabilization. Au_{10} is carrying out this latter action more efficiently than the smaller Au_3, which explains its larger activity.

In a study based on ab initio molecular dynamics simulations (AIMD) and micro-kinetic modeling, Wang et al.[146] suggested a mechanism for CO oxidation involving oxidized Au^+ species at the borders of TiO_2-supported Au_{20} clusters. After oxygen adsorption on the gold cluster, oxidized O_{ad}-Au^+ species forms and adsorbs CO. In turns, the abstraction of a vicinal lattice O species to form CO_2 results favored.

Recently, DFT calculations performed on an Au nano-rod supported on a TiO_2 anatase (101) substrate confirmed their role in facilitating the formation of the oxygen vacancies, resulting in a moderate barrier for the MvK mechanism (0.9 eV).[147]

MvK mechanisms mediated by lattice oxygen species were also reported for other reducible oxides, for instance in the case of Au_{12} particles supported on ceria.[148] Hoh et al. observed that, in presence of Au nanoparticles, the oxygen vacancy formation energy on the Fe_2O_3(001) surface decreased by almost 30%.[149]

It is thus proven that the reducible character of the oxide allows the lattice oxygen to take side in oxidation reactions via the MvK mechanism. Nevertheless, such a process was reported also for non-reducible oxides, thanks to enabling role of the supported gold particles in creating oxygen vacancies. In the case of Au/ZrO_2, a DFT study proposed a three-step mechanism (Figure 4):[150] i) a CO molecule reacts with a lattice O at the Au/oxide interface, with a barrier of 0.79 eV; ii) the interface is also active toward the dissociation of the oxygen molecule (0.33 eV) and the refilling of the vacancy (0.43 eV); iii) a second CO molecule reacts with the remaining oxygen adatom, restoring the catalyst (barrier of 0.81 eV). A key aspect supporting this mechanism is that the vacancy formation energy at the Au/ZrO_2 interface is less than half compared to bare zirconia.

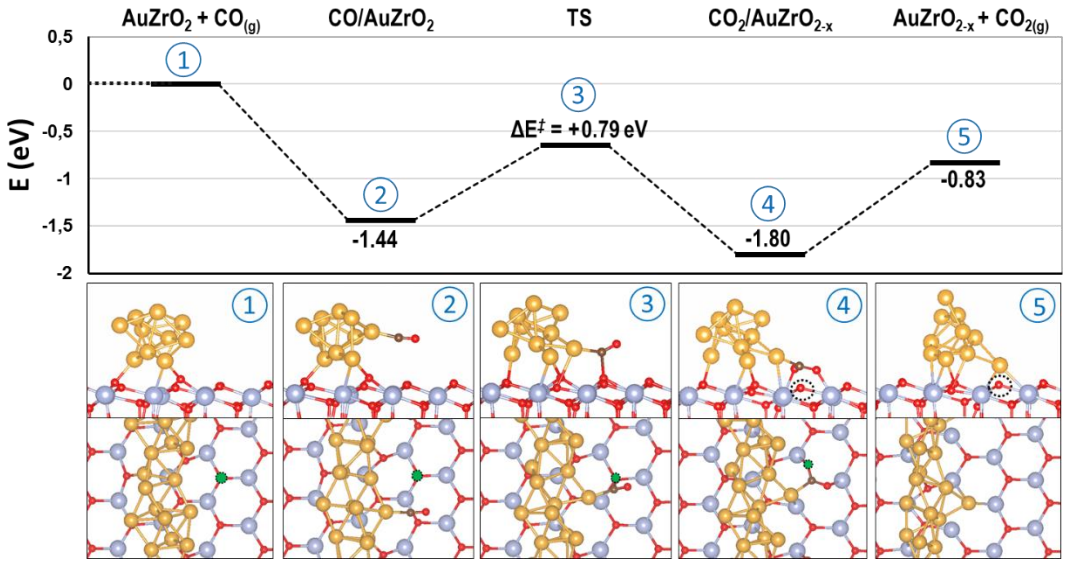

Figure 4. (top) Reaction energy profile and (bottom) side and top view of the structures of the CO oxidation reaction with a surface O_{latt}. The O_{latt} abstracted is indicated by a green filled circle, and the O vacancy by a dotted circle. Zr is represented by blue atoms, O by red atoms, Au by golden atoms, and C by brown atoms. Reprinted with permission from ref. 150. Copyright (2017) Wiley-VCH Verlag GmbH&Co. KGaA, Weinheim.

.

In the case of MgO, finally, whose very large band gap and substantial ionic character hinder the formation of oxygen vacancies, a LH mechanism enabled by supported gold particles was reported by DFT calculations.[151,152] Also in this case, the undercoordinated Au and Mg sites at the Au/MgO interface were indicated as the most favorable sites for the reactions.

4.2 Other reactions

The activity of Au clusters and particles in several organic reactions was scanned by means of first-principle simulations.[153-155] We hereby analyse few selected examples.

Phan et al.[156] have recently reviewed the role of supported Au-clusters in catalytic H_2 production via the water-gas-shift (WGS) reaction, where CO reacts with water to form hydrogen and CO_2:

$CO + H_2O \rightarrow H_2 + CO_2$

The most studied model systems for this reaction are Pt and Au clusters supported on reducible oxides, such as titania or ceria. At variance from the CO oxidation case, here no direct participation of lattice oxygen ions in the reaction is envisaged. Nevertheless, reducibility is once again a desirable feature for the supporting oxide, since oxygen vacancies are ideal anchoring sites for the metal particles, preventing sintering.[157] Other DFT calculations evidenced that, on reducible supports, the Au adhesion energy is enhanced by the formation of an O-rich/$Au^{\delta+}$ interface.[158]

An aspect that deserves to be elucidated is why Au/CeO_2 outperforms Au/TiO_2 in WGS activity.[159] Several computational papers provide a roadmap to understand this finding, based on the different strength of the Au/support interaction (vide supra). on titania, gold particles are weakly bound, without substantial charge transfer.[158-161] On ceria, the stronger interaction and the substantial charge transfer perturb and activate the metal particle, which may increase the activity toward OH bond cleavage and WGS reaction.[114,162]

The Au/TiO_2 system has also been widely employed as a photocatalyst for WGS reaction. The role of the metal particle in the photocatalytic process is not trivial to account for. On the one hand, gold particles under irradiation show

plasmonic behaviour, and the collective excitation of their electrons facilitate the transfer of the photoexcited electrons in the TiO_2 conduction band, preventing the recombination between photoexcited electrons and holes in the oxide.[163] The photoexcited holes, in turns, oxidize the hydroxyl groups favouring the hydrogen formation. The higher the metal's work function, the larger the Schottky barrier preventing recombination,[164] which explains why noble metals (Au or Pt) are often used in these photocatalytic devices. According to an alternative model, the gold particles act as a recombination centre where H radical species arising from water splitting combine into H_2 molecules, Figure 5.[165]

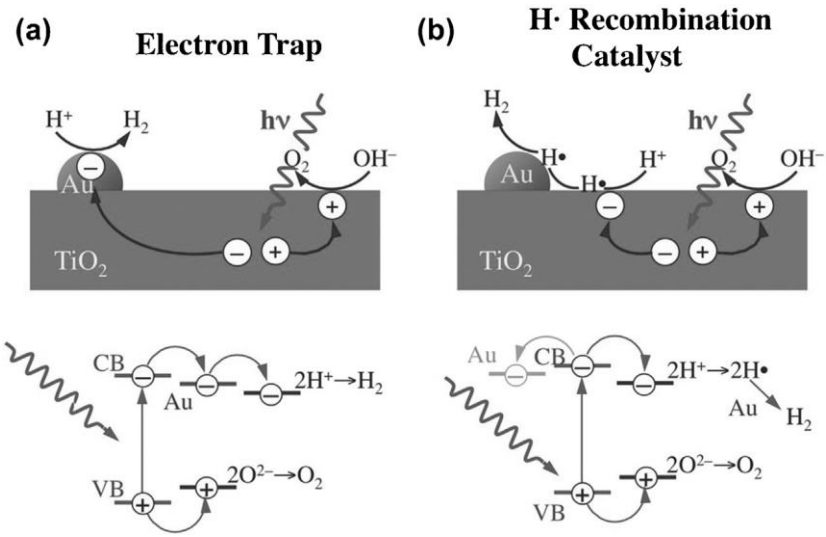

Figure 5. Proposed mechanisms and electronic transitions to explain the role of Au NPs in the photocatalytic water splitting with TiO_2: (a) Au nanoparticles acts as an electron trap that physically separates the excited electron used for proton reduction from the oxidation step that occurs on the TiO_2 surface; (b) H^+ reduction occurs at TiO_2 sites but that the resulting hydrogen atoms need to migrate to Au NPs to recombine and produce H_2 product. Reprinted with permission from Joo et al.[165] Copyright (2014) National Academy of Sciences.

The hydrogenation of CO_2 to methanol is a reaction of paramount relevance under the environmental point of view, since it directly converts a pollutant into a valuable chemical product. The activation of carbon dioxide, however, is a particularly hard task, due to the high thermodynamic stability of the CO_2 molecule. Once again, the combination of noble metal small particles and oxide surfaces is a system at the key of the catalytic processes enabling this reaction.

It has been proposed that activation of CO_2 occurs at the oxide support or at the interfacial sites between the active metal and the oxide support.[166] As experimentally proven by Haruta et al.,[167] the choice of the support is critical: while Au/TiO_2 results more active, Au/CeO_2 has a better selectivity. Indeed, it has been widely reviewed in the literature how the basicity and reducibility of an oxide strongly increases its capability to activate the C-O bond, which explains why titania and ceria are good candidates.[160,161,168-171]

An intriguing possibility to explore is the formation of oxide-oxide junctions, to tune the catalytic properties of the oxidic support. In the case of a titania/ceria interface, the most interesting junction's effect concerns the stabilization of Ce^{3+} centres, thus further increasing ceria's reducibility.[172] Strongly reduced ceria will, in turns, transfer some charge to supported gold clusters, contributing to their activation, as shown in a joint computational-experimental work, [173] where CO_2 hydrogenation to methanol on gold clusters supported on titania/ceria interfaces is studied. The rutile (110) surface was adopted as model for titania, while the titania/ceria interface was modelled adsorbing Ce_2O_3 dimers on it, Figure 6 A.[173] On both TiO_2 and CeO_x/TiO_2 model systems, Au_3 clusters were deposited, simulating the metal dispersed active phase. Interestingly, the titania/ceria composite binds strongly the gold aggregates also in absence of oxygen vacancies, which is not the case for the pristine oxides. The increased binding of Au on CeO_x/TiO_2 is attributed to the presence of Ce^{3+} cations. The reduced character of the ceria adducts induces a remarkable charge transfer to the gold aggregate,

which makes it reactive towards CO_2, with the positive pole of the molecule binding to $Au^{\delta-}$, while the negatively charged oxygen binds to $Ce^{\delta+}$. The potential energy surfaces for TiO_2 and CeO_x/TiO_2 supports are compared in Figure 6B. On both supports, the reaction proceeds via reverse water-gas shift leading to CO via *HOCO intermediates followed by CO hydrogenation to methanol via *HCO, $*H_2CO$, and $*H_3CO$ intermediates. Despite the similarity in the mechanism, the initial activation barrier for CO_2 is one order of magnitude smaller on CeO_x/TiO_2 support compared to bare titania. The barrier for the last hydrogenation step, the conversion of methoxy species to methanol, is also decreased by the presence of ceria, which may explain the improvement on the selectivity to methanol observed experimentally.[167] It is worth noting that the key-steps of the reaction occur at the metal–oxide interface sites.

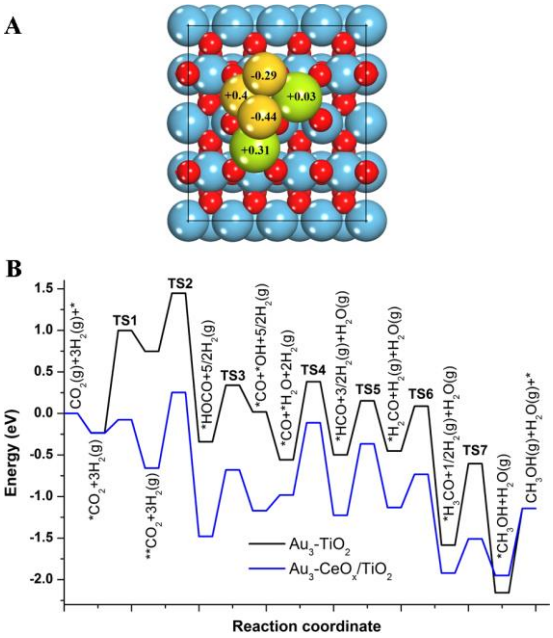

Figure 6. Charge transfer and reaction energetics calculated by DFT. (A) The net Bader charges of Au and Ce; $^+$ indicates electron loss; $^-$ indicates electron gain. (B) DFT-optimized potential energy surface (PES) for CO_2 hydrogenation on $Au_3/TiO_2(110)$ and $Au_3/CeO_x/TiO_2(110)$. "TS" corresponds to transition state. Reprinted with permission from ref. 173. Copyright (2015) American Chemical Society.

Conclusions

Far from being exhaustive on the very, very wide topic of DFT studies of oxide surfaces from the fundamental point view, as well as their catalytic application, this short overview hopefully provides to the readers a few critical hints on some aspects.

The key-descriptors of the catalytic processes on oxide-supported metallic heterogeneous catalysts are the creation of point defects and the structural and electronic rearrangements induced at the cluster oxide interface. It is worth noting that these are real challenges for simulations, in particular the estimation of the charge transfer. This implies a careful validation of the adopted methodology, ensuring that i) the electronic structure of both the metal oxide and the supported metal particles are simultaneously well described ii) the formation energy of the point defects is physically sound iii) the model structure correctly accounts for the structural constrains and long-range electrostatic effects (if a cluster approach is adopted). Nevertheless, DFT calculations still represent a tool of paramount relevance to unravelling the mechanistic aspects of the catalytic reactions, and their relationship with the structure and chemical nature of the support.

[1] C. Sousa, S. Tosoni, F. Illas, Chem Rev. 113 (2013) 4456

[2] R. Runge, E. K. U. Gross, Phys. Rev. Lett. 52 (1984) *52*

[3] G. Onida, L. Reining, A. Rubio, Rev. Mod. Phys. 74 (2002) 601

[4] C. A. Ulrich *Time-Dependent Density-Functional Theory: Concepts and Applications*; Oxford University Press Inc.: Oxford, UK, 2012

[5] M. A. L. Marques, E. K. U. Gross, Annu. Rev. Phys. Chem. 55 (2004) 427

[6] F. Furche, R. Ahlrichs, J. Chem. Phys. 117 (2002) 7433

[7] A. F. Izmaylov, G. E. J. Scuseria, Chem. Phys. 129 (2008) 034101

[8] D. Jacquemin, B. Mennucci, C. Adamo, Phys. Chem. Chem. Phys. 13 (2011) 16987

[9] R. Dovesi, V. R. Saunders, C. Roetti, R. Orlando, C. M. Zicovich-Wilson, Pascale, F.; B. Civalleri, K. Doll, N. M. Harrison, I. J. Bush, Ph. D'Arco, M. Llunell, *CRYSTAL2006, User's Manual*.; University of Torino: Torino, Italy, 2006

[10] B. Civalleri, D. Presti, R. Dovesi, A. Savin, Chem. Modell. 9 (2012) 168

[11] J. He, C. Franchini, J. Phys.: Condens. Matter 29 (2017) 454004

[12] M. Gerosa, C.E. Bottani, C. Di Valentin, G. Onida, G. Pacchioni, J. Phys.: Condens. Matter 30 (2017) 044003

[13] J. Heyd, J. E. Peralta, G. E. Scuseria, J. Chem. Phys. 123 (2005) 174101

[14] F. Tran, P. Blaha, J. Phys. Chem. A 121 (2017) 3318

[15] P. Borlido, T. Aull, A. W. Huran, F. Tran, M. A. L. Marques, S. Botti, J. Chem. Theory Comput. 15 (2019) 5069

[16] J. P. Perdew, W. Yang, K. Burke, Z. Yang, E. K. U. Gross, M. Scheffler, G. E. Scuseria, T. M. Henderson, I. Y. Zhang, A. Ruzsinszky, H. Peng, J. Sun, E. Trushin, A. Görling PNAS 114 (2017) 2801

[17] T. Das, G. Di Liberto, S. Tosoni, G. Pacchioni, J. Chem. Theory Comput. 15 2019, 6294

[18] Y. Hinuma, Y. Kumagai, I. Tanaka, F. Oba, Phys. Rev. B 95 (2017) 075302

[19] T. Shimazaki, Y. Asai, Phys. Lett. 466 (2008) 91

[20] A. lkauskas, P. Broqvist, A. Pasquarello, Phys. Status Solidi B 248 (2011) 775

[21] A. I. Liechtenstein, V. I. Anisimov, J. Zaanen, Phys. Rev. B 52 (1995) R5467

[22] V. I. Anisimov, F. Aryasetiawan, A.I. Lichtenstein, J. Phys.: Condens. Matt. 9 (1997) 767

[23] M. Cococcioni, S. de Gironcoli, Phys. Rev. B 71 (2005) 035105.

[24] H. J. Kulik, M. Cococcioni, D.A. Scherlis, N. Marzari, Phys. Rev. Lett. 97 (2006) 103001

[25] N. J. Mosey, E. A. Carter, Phys. Rev. B 76 (2007) 155123

[26] G. Pacchioni, G. Cogliandro, P.S. Bagus, Int. J. Quantum Chem. 42 (1992) 1115

[27] G. Pacchioni, J. M. Ricart, F. Illas, J. Am. Chem. Soc. 116 (1994) 10152

[28] M. A. Nygren, L. G. M. Pettersson, Z. Barandiaran, L. Seijo, J. Chem. Phys. 100 (1994) 2010

[29] N. W. Winter, R. M. Pitzer, D. K. Temple, J. Chem. Phys. 86 (1987) 3549

[30] N. W. Winter, R. M. Pitzer, J. Chem. Phys. 89 (1988) 446

[31] Z. Barandiarán, L. Seijo, J. Chem. Phys. 89 (1988) 5739

[32] L. Seijo, Z. Barandiarán, *Computational Chemistry: Reviews of Current Trends*; World Scientific: Singapore, 1999.

[33] J. L. Pascual, N. Barros, Z. Barandiaran, L. Seijo, J. Phys. Chem. A 113 (2009) 12454

[34] P. P. Ewald, Ann. Physik 64 (1921) 253

[35] H. M. Evjen, Phys. Rev. 39 (1932) 675

[36] P. Reinhardt, M. P. Habas, R. Dovesi, I. de P.R. Moreira, F. Illas, Phys. Rev. B 59 (1999) 1016

[37] J. R.B. Gomes, F. Illas, N.C. Hernandez, J.F. Sanz, A. Wander, N.M. Harrison, J. Chem. Phys. 116 (2002) 1684

[38] J. R.B. Gomes, F. Illas, N.C. Hernandez, A. Marquez, J.F. Sanz, Phys. Rev. B 65 (2002) 125414

[39] J. R. B. Gomes, Z. Lodziana, F. Illas, J. Phys. Chem. B 107 (2003) 6411

[40] M. Born, Z. Physik 1 (1929) 45

[41] B. G. Dick, A. W. Overhauser, Phys. Rev. 112 (1958) 90

[42] C. R. A. Catlow, M. Dixon, W.C. Mackrodt, in: *Computer Simulation of Solids*; Catlow, C. R. A. (ed.), Springer, Berlin, 1982

[43] A. L. Shluger, P.V. Sushko, L.N. Kantorovich, Phys. Rev. B 59 (1999) 2417

[44] A. L. Shluger, A. H. Harker, V. E. Puchin, N. Itoh, C. R. A. Catlow, Model. Simul. Mater. Sci. Eng. 1 (1993) 673

[45] A. L. Shluger, J. D. Gale, Phys. Rev. B 54 (1996) 962

[46] V. A. Nasluzov, E. A. Ivanova, A. M. Shor, G. N. Vayssilov, U. Birkenheuer, N. Rosch, J. Phys. Chem. B 107 (2003) 2228

[47] V. A. Nasluzov, V. V. Rivanenkov, A. B. Gordienko, K. M. Neyman, U. Birkenheuer, N. Rosch, J. Chem. Phys. 115 (2001) 8157

[48] K. M. Neyman, C. Inntam, V. A. Nasluzov, R. Kosarev, N. Rösch, Appl. Phys. A 78 (2004) 823.

[49] V.A. Nasluzov, V.V. Rivanenkov, A.M. Shor, K.M. Neyman, N. Rösch, Chem. Phys. Lett. 374 (2003) 487

[50] V.V. Rivanenkov, V.A. Nasluzov, A.M. Shor, K.M. Neyman, N Rösch, Surf. Sci. 525 (2003) 173

[51] L. V. Moskaleva, V.A. Nasluzov, Z.X. Chen, N. Rösch, Phys. Chem. Chem. Phys. 6 (2004) 4505

[52] E. A. I. Shor, A. M. Shor, V. A. Nasluzov, G. N. Vayssilov, N. Rösch, J. Chem. Theory Comput. 1 (2005) 459

[53] V. A. Nasluzov, T.V. Shulimovich, E.A.I. Shor, A.M. Shor, N. Rösch, Chem. Phys. Lett. 494 (2010) 243

[54] J. Sauer, P. Ugliengo, E. Garrone, V.R. Saunders, Chem. Rev. 94 (1994) 2095

[55] G. Pacchioni, Heter. Chem. Rev. 2 (1995) 213

[56] P.S. Bagus, F. Illas, in The Surface Chemical Bond in Schleyer, P.V.; Allinger, N.L.; Clark, T.; Gasteiger, J.; Kollman, P.A.; Schaefer III, H.F.; Schreiner, P.R. (eds.) Encyclopedia of Computational Chemistry; John Wiley & Sons: Chichester, U.K., 1998, p.2870

[57] H. Lin, D.G. Truhlar, Theor. Chem. Acc. 117 (2007) 185

[58] F. Maseras, K. Morokuma, J. Comput. Chem. 16 (1995) 1170

[59] M. Svensson, S. Humbel, R.D.J. Froese, T. Matsubara, S. Sieber, K. Morokuma, J. Phys. Chem. 100 (1996) 19357

[60] N. Lopez, G. Pacchioni, F. Maseras, F. Illas, Chem. Phys. Lett. 294 (1998) 611

[61] M. Boronat, P.M. Viruela, A. Corma, J. Am. Chem. Soc. 126 (2004) 3300

[62] S. Kasuriya, S. Namuangruk, P. Treesukol, M. Tirtowidjojo, J. Limtrakul, J. Catal. 219 (2003) 320

[63] S. Namuangruk, P. Pantu, J. Limtrakul, J. Catal. 225 (2004) 523

[64] X. Solans-Monfort, M. Sodupe, V. Branchadell, J. Sauer, R. Orlando, P. Ugliengo, J. Phys. Chem. B 109 (2005) 3539

[65] I. Roggero, B. Civalleri, P. Ugliengo, Chem. Phys. Lett. 341 (2011) 625

[66] A. Damin, S. Bordiga, A. Zecchina, C. Lamberti, J. Chem. Phys. 117 (2002) 226

[67] K. Bobuatong, J. Limtrakul, Appl. Catal. A 253 (2003) 49

[68] S. Wannakao, P. Khongpracha, J. Limtrakul, J. Phys. Chem. A 115 (2011) 12486

[69] S. Jungsuttiwong, J. Lomratsiri, J. Limtrakul, Int. J. Quantum Chem. 111 (2011) 2275

[70] T. Maihom, P. Pantu, C. Tachakritikul, M. Probst, J. Limtrakul, J. Phys. Chem. C 114 (2010) 7850

[71] Y. Perez-Badell, X. Solans-Monfort, M. Sodupe, L.A. Montero, Phys. Chem. Chem. Phys. 12 (2010) 442

[72] C. Kumsapaya, K. Bobuatong, P. Khongpracha, Y. Tantirungrotechai, J. Limtrakul, J. Phys. Chem. C 113 (2009) 16128

[73] C.Y. Sung, L.J. Broadbelt, R.Q. Snurr, J. Phys. Chem. C 113 (2009) 15643

[74] T. Maihom, B. Boekfa, J. Sirijaraensre, T. Nanok, M. Probst, J. Limtrakul, J. Phys. Chem. 113 (2009) 6654

[75] P. Sherwood, A.H. de Vries, M.F. Guest, G. Schreckenbach, C.R.A. Catlow, S.A. French, A.A. Sokol, S.T. Bromley, W. Thiel, A.J. Turner, S. Billeter, F. Terstegen, S. Thiel, J. Kendrick, S.C. Rogers, J. Casci, M. Watson, F. King, E. Karlsen, M. Sjovoll, A. Fahmi, A- Schafer, C. Lennartz, J. Mol. Struct. Theochem 632 (2003) 1

[76] G. Kresse, J. Hafner, Phys. Rev. B 47 (1993) 558

[77] G. Kresse, J. Furthmüller, Comput. Mater. Sci. 6 (1996) 15

[78] G. Kresse, J. Furthmüller, Phys. Rev. B 54 (1996) 11169

[79] M.D. Segall, P.J.D. Lindan, M.J. Probert, C.J. Pickard, P.J. Hasnip, S.J. Clark, M.C. Payne, J. Phys.: Condens. Matter 14 (2002) 2717

[80] X. Gonze, J.M. Beuken, R. Caracas, F. Detraux, M. Fuchs, G.M. Rignanese, L. Sindic, M. Verstraete, G. Zerah, F. Jollet, M. Torrent, A. Roy, M. Mikami, P. Ghosez, J.Y. Raty, D.C. Allan, Comput. Mat. Sci. 25 (2002) 478

[81] X. Gonze, B. Amadon, P.M. Anglade, J.M. Beuken, F. Bottin, P. Boulanger, F. Bruneval, D. Caliste, R. Caracas, M. Cote, T. Deutsch, L. Genovese, P. Ghosez, M. Giantomassi, S. Goedecker, D.R. Hamann, P. Hermet, F. Jollet, G. Jomard, S. Leroux, M. Mancini, S. Mazevet, M.J.T. Oliveira, G. Onida, Y. Pouillon, T. Rangel, G.M. Rignanese, D. Sangalli, R. Shaltaf, M. Torrent, M.J. Verstraete, G. Zerah, J.W. Zwanziger, Comput. Phys. Comm. 180 (2009) 2582

[82] P. Giannozzi, S. Baroni, N. Bonini, M. Calandra, R. Car, C. Cavazzoni, D. Ceresoli, G.L. Chiarotti, M. Cococcioni, I. Dabo, A. Dal Corso, S. de Gironcoli, S. Fabris, G. Fratesi, R. Gebauer, U. Gerstmann, C. Gougoussis, A. Kokalj, M. Lazzeri, L. Martin-Samos, N. Marzari, F. Mauri, R. Mazzarello, S. Paolini, A. Pasquarello, L. Paulatto, C. Sbraccia, S. Scandolo, G. Sclauzero, A.P. Seitsonen, A. Smogunov, P. Umari, R.M. Wentzcovitch, J. Phys.: Condens. Matt. 21 (2009) 395502

[83] Z. Ma, F. Zaera "Heterogeneous Catalysis by Metals" in "Encyclopedia of Inorganic Chemistry", John Wiley & Sons, New York, USA, 2006

[84] I. Chorkendorff, J. W. Niemantsverdriet, "Concepts of Modern Catalysis and Kinetics", John Wiley & Sons, New York, USA, 2017

[85] S. Schauermann, N. Nilius, S. Shaikhutdinov, H.-J. Freund Acc. Chem. Res. 46 (2013) 1673

[86] A. Bell, Science 299 (2003) 1688

[87] M Valden, X. Lai, D.W. Goodman Science 281 (1998) 1647

[88] A. Sanchez, S. Abbet, U. Heiz, W.-D. Schneider, H. Häkkinen, R. N. Barnett, and U. Landman J. Phys. Chem. A 103 (1999) 9573

[89] E. Bus, R. Prins, J. A. van Bokhoven, Catal. Commun. 8 (2007) 1397

[90] A. Ruiz, P. Schlexer, S. Tosoni, G. Pacchioni, ACS Catal. 7 (2017) 6493

[91] S. J. Tauster, Acc. Chem. Res. 20 (1987) 389

[92] O. Dulub, W. Hebenstreit, U. Diebold Phys. Rev. Lett. 84 (2000) 3646

[93] Z.-H. Qin, M. Lewandowski, Y.-N. Sun, S. Shaikhutdinov, H.-J. Freund J. Phys. Chem. C 112 (2008) 10209

[94] F. Polo-Garzon, T. F. Blum, Z. Bao, K. Wang, V. Fung, Z. Huang, E. E. Bickel, D. Jiang, M. Chi, Z. Wu, ACS Catal. 11 (2021) 1938

[95] M. Lewandowski, Y.N. Sun, Z.-H. Qin, S. Shaikhutdinov, H.-J. Freund Appl. Catal. A 391 (2011) 407

[96] S. Tosoni, G. Pacchioni, ChemCatChem 11 (2019) 73

[97] G. Ertl, H. Knözinger, F. Schueth, J Weitkamp, Handbook of Heterogeneous Catalysis, 2nd ed Wiley-VCH, Weinheim, 2008.

[98] M. Haruta, N. Yamada, T. Kobayashi, S. Iijima, J. Catal. 115 (1989) 301

[99] M. Haruta, Cattech 6 (2002) 102

[100] T. P. St. Clair, D. W. Goodman, Top. Catal. 13 (2000) 5

[101] B. E. Hayden, D. Pletcher, M. E. Rendall, J. P. Suchsland, J. Phys. Chem. C 111 (2007) 17044

[102] T. Risse, S. Shaikhutdinov, N. Nilius, M. Sterrer, H.-J. Freund, Acc. Chem. Res. 41 (2008) 949

[103] C. T. Campbell, Surf. Sci. Rep. 27 (1997) 1

[104] R. Narayanan, M.-A. El-Sayed, J. Am. Chem. Soc. 125 (2003) 8340

[105] K. Bang, K. Shin, M. S. Ryu, S. Kwon, H. M. Lee, Catal. Today 265 (2016) 14

[106] P. Schlexer, G. Pacchioni, J. Phys. Chem. C 121 (2017) 14717

[107] B. Yang, Y. Pan, X. Lin, N. Nilius, H.-J. Freund, C. Hulot, A. Giraud, S. Blechert, S. Tosoni, J. Sauer, J. Am. Chem. Soc. 134 (2012) 11161

[108] S. Hemmingson, C. T. Campbell, ACS Nano 11 (2017) 1196

[109] C. T. Campbell, J. R. V. Sellers, Faraday Discuss. 162 (2013) 9

[110] L. Xu, G. Henkelman, C. T. Campbell, H. Jónsson, Phys. Rev. Lett. 95 (2005) 146103

[111] M. M. Branda, N. C. Hernández, J. F. Sanz, J. Phys. Chem. C 114 (2010) 1934

[112] S. Ferndandez, A. Markovits, C. Minot, Chem. Phys. Lett. 463 (2008) 106

[113] S. Sicolo, L. Giordano, G. Pacchioni, J. Phys. Chem. C 113 (2009) 16694

[114] J. A. Rodriguez, J. Evans, J. Graciani, J. B. Park, P. Liu, J. Hrbek, J. F. Sanz, J. Phys. Chem. C 113 (2009) 7364

[115] S. Tosoni, G. Pacchioni, J. Phys. Chem. C 121 (2017) 28328

[116] "Adsorption on Ordered Surfaces of Ionic Solids and Thin Films", Proceedings of 106th WE-Heraeus Seminar, Bad Honnef (Eds.: H.J. Freund, E. Umbach), Springer, Berlin, 1993.

[117] V. E. Henrich, P. A. Cox, The Surface Science of Metal Oxides Cambridge University Press, Cambridge, UK, 1994.

[118] T. König, G. H. Simon, U. Martinez, L. Giordano, G. Pacchioni, M. Heyde, H.-J. Freund, ACS Nano 4 (2010) 2510

[119] A. Sanchez, S. Abbet, H. Heiz, W. D. Schneider, H. Häkkinen, R. N. Barbett, U. Landman, J. Phys. Chem. A 103 (1999) 9573

[120] B. Yoon, H. Häkkinen, U. Landman, A. S. Wörz, J. M Antonietti, S. Abbet, K. Judai, U. Heiz, Science 307 (2005) 403

[121] S. Chrétien, H. Metiu, J. Chem. Phys. 126 (2007) 104701

[122] N. Nilius, V. Brázdová, M. -V. Ganduglia-Pirovano, V. Simic-Milosevic, J. Sauer, H. -F. Freund, New J. Phys. 11 (2009) 093007

[123] P. Schlexer, G. Pacchioni, Top. Catal. 60 (2017) 459

[124] X. Shao, S. Prada, L. Giordano, G. Pacchioni, N. Nilius, H.-J. Freund, Angew. Chem. Int. Ed. 50 (2011) 11525

[125] F. Stavale, X. Shao, N. Nilius, H.-J. Freund, S. Prada, L. Giordano, G. Pacchioni, J. Am. Chem. Soc. 134 (2012) 11380

[126] S. Prada, L. Giordano, G. Pacchioni, J. Phys.: Condens. Matter 26 (2014) 315004

[127] G. Pacchioni, Cat. Lett. 145 (2015) 80

[128] J. Paier, M. Marsman, G. Kresse, J. Chem. Phys. 127 (2007) 024103

[129] J. Paier, M. Marsman, K. Hummer, G. Kresse, J. Chem. Phys. 124 (2006) 154709

[130] K. Honkala, H. Häkkinen, J. Phys. Chem. C 111 (2007) 4319

[131] S. C. Ammal, A. Heyden, J. Chem. Phys. 133 (2010) 164703

[132] R. Coquet, K. L. Howard, D. J. Willock, Chem. Soc. Rev. 37 (2008) 2046

[133] M. Okumura, J. M. Coronado, J. Soria, M. Haruta, J. Conesa, J. Catal. 203 (2001) 168

[134] Z. P. Liu, X. Q. Gong, J. Kohanoff, C. Sanchez, P. Hu, Phys. Rev. Lett. 91 (2003) 266102

[135] I.N. Remediakis, N. Lopez, J. Nørskov, Angew. Chem.: Int. Ed. 44 (2005) 1824

[136] L. M. Molina, B. Hammer, Appl. Catal. A: General 291 (2005) 21

[137] J. Gong, C. B. Mullins, Acc. Chem. Res. 42 (2009) 1063

[138] M. Kotobuki, R. Leppelt, D. A. Hansgen, D. Widmann, R. J. Behm, J. Catal. 264 (2009) 67

[139] D. Widmann, R. J. Behm, Angew. Chem. Int. Ed. 50 (2011) 10241

[140] D. Widmann, Y. Liu, F. Schüth, R. J. Behm, J. Catal. 276 (2010) 292

[141] D. Widmann, R. J. Behm, Acc. Chem. Res. 47 (2014) 740

[142] L. Li, X. C. Zeng, J. Am. Chem. Soc. 136 (2014) 15857

[143] L. Li, Y. Gao, H. Li, Y. Zhao, Y. Pei, Z. F. Chen, X. C. Zeng, J. Am. Chem. Soc. 135 (2013) 19336

[144] M. A. Saqlain, A. Hussain, M. Siddiq, A. R. Ferreira, A. A. Leitão, Phys. Chem. Chem. Phys. 17 (2015) 25403

[145] M. A. Saqlain, A. Hussain, M. Siddiq, A. A. Leitão, Appl. Catal. A: General 519 (2016) 27

[146] Y. G. Wang, D. C. Cantu, M. S. Lee, J. Li, V. A. Glezakou, R. Rousseau, J. Am. Chem. Soc. 138 (2016) 10467

[147] P. Schlexer, D. Widmann, J. Behm, G. Pacchioni ACS Catalysis 8 (2018) 6513

[148] H. Y. Kim, G. Henkelman, J. Phys. Chem. Lett. 4 (2013) 216

[149] S. W. Hoh, L. Thomas, G. Jones, D. J. Willok, Rev. Chem. Intermed. 41 (2015) 9587

[150] A. Ruiz-Puigdollers, G. Pacchioni, ChemCatChem 9 (2017) 1119

[151] L. M. Molina, B. Hammer, Phys. Rev. Lett. 90 (2003) 206102

[152] L. M. Molina, B. Hammer, Phys. Rev. B 69 (2004) 69 155424

[153] A. Abad, P. Concepcion, A. Corma, H. Garcia, Angew. Chem., Int. Ed. 44 (2005) 4066

[154] A. Abad, C. Almela, A. Corma, H. Garcia, Chem. Commun. (2006) 3178

[155] S. Lee, L. M. Molina, M. J. Lopez, J. A. Alonso, B. Hammer, B. Lee, S. Seifert, R. E. Winans, J. W. Elam, M. J. Pellin, et al., Angew. Chem., Int. Ed. 48 (2009) 1467

[156] T.-D. Nguyen-Phan, A. E. Baber, J. A. Rodriguez, S. D. Senanayake, Appl. Catal. A: General 518 (2016) 18

[157] R. P. Galhenage, H. Yan, S. A. Tenney, N. Park, G. Henkelman, P. Albrecht, D. R. Mullins, D. A. Chen, J. Phys. Chem. C 117 (2013) 7191

[158] D. Matthey, J. G. Wang, S. Wendt, J. Matthiesen, R. Schaub, E. Lægsgaard, B. Hammer, F. Besenbacher, Science 315 (2007) 1692

[159] J. A. Rodriguez, P. Liu, J. Hrbek, J. Evans, M. Pérez, Angew. Chem.: Int. Ed. 46 (2007) 1329

[160] J. B. Park, J. Graciani, J. Evans, D. Stacchiola, S. Ma, P. Liu, A. Nambu, J. F. Sanz, J. Hrbek, J. A. Rodriguez, Proc. Natl. Acad. Sci. U. S. A. 106 (2009) 4975

[161] J. B. Park, J. Graciani, J. Evans, D. Stacchiola, S. D. Senanayake, L. Barrio, P. Liu, J. Fdez. Sanz, J. Hrbek, J. A. Rodriguez, J. Am. Chem. Soc. 132 (2010) 356

[162] H. Iddir, S. Öğüt, N. D. Browning, M. M. Disko, Phys. Rev. B 73 (2006) 039902

[163] G. L. Chiarello, M. H. Aguirre, E. Selli, J. Catal. 273 (2010) 182

[164] M. Jakob, H. Levanon, P. V. Kamat, Nano Lett. 3 (2003) 353

[165] J. B. Joo, R. Dillon, I. Lee, Y. Yin, C. J. Bardeen, F. Zaera, Proc. Natl. Acad. Sci. U. S. A. 111 (2014) 7942

[166] D. Pakhare, J. Spivey, Chem. Soc. Rev. 43 (2014) 7813

[167] H. Sakurai, S. Tsubota, M. Haruta, Appl. Catal. A: General 102 (1993) 125

[168] Z. Zhang, X. Verykios, Catal. Lett. 38 (1996) 175

[169] T. Staudt, Y. Lykhach, N. Tsud, T. Skála, K. C. Prince, V. Matolín, J. Libuda, J. Phys. Chem. C 115 (2011) 8716

[170] A. Trovarelli, Catal. Rev.: Sci. Eng. 38 (1996) 439

[171] K. Zhou, Z. Yang, S. Yang, Chem. Mater. 19 (2007) 1215

[172] J. Graciani, J. J. Plata, J. F. Sanz, P. Liu, J. A. Rodriguez, J. Chem. Phys. 132 (2010) 104703

[173] X. Yang, S. Kattel, S. D. Senanayake, J. A. Boscoboinik, X. Nie, J. Graciani, J. A. Rodriguez, P. Liu, D. J. Stacchiola, J. G. Chen, J. Am. Chem. Soc. 137 (2015) 10104